Prospects for $\gamma\,\gamma \to H$ and $\gamma\,\gamma \to W^+W^-$ measurements at the FCC-ee

Patricia Rebello Teles
Centro Brasileiro de Pesquisas Fisicas - CBPF
22290-180 Rio de Janeiro, Brazil
E-mail: patricia.rebello.teles@cern.ch

David d'Enterria
CERN, PH Department
1211 Geneva, Switzerland
E-mail: dde@cern.ch

Abstract. We study the possibilities for the measurement of two-photon production of the Higgs boson (in the $b\bar{b}$ decay channel), and of W^+W^- pairs (decaying into four jets) in e^+e^- collisions at the the Future Circular Collider (FCC-ee). The processes are simulated with the PYTHIA and MADGRAPH 5 Monte Carlo codes, using the effective photon approximation for the e^+e^- photon fluxes, at center-of-mass energies $\sqrt{s} = 160$ GeV and 240 GeV. The analyses include electron-positron tagging, realistic acceptance and reconstruction efficiencies for the final-state jets, and selection criteria to remove the backgrounds. Observation of both channels is achievable with the expected few ab^{-1} integrated luminosities at FCC-ee.

1. Introduction

After the LHC discovery of the Higgs boson with properties consistent with the standard model (SM) expectations [1], the priority in high-energy particle physics is more-than-ever focused on looking for evidences of "new physics" that can help explain the many fundamental problems still open in the field (nature of dark matter, matter-antimatter asymmetry, unnatural gap between the electroweak and Planck scales,...). At CERN, the design study of the Future Circular Collider (FCC) has been launched to pursue the searches of physics beyond the SM in a new 80–100 km tunnel once the LHC research project is completed [2]. Running in its first phase as a very-high-luminosity electron-positron collider, the FCC-ee (formerly known as TLEP [3]) will provide unique possibilities for indirect searches of new phenomena through high-precision tests of the SM by collecting tens of ab^{-1} integrated luminosities at the Z pole ($\sqrt{s} = 91$ GeV), the W-pair production threshold ($\sqrt{s} = 160$ GeV), the HZ Higgs-strahlung maximum around $\sqrt{s} = 240$ GeV, and the $t\bar{t}$ threshold ($\sqrt{s} = 350$ GeV).

Beyond the rich physics programme in electron-positron collisions, the FCC-ee will provide an ideal environment to study $\gamma\,\gamma$ collisions at unprecedented energies and luminosities. Though photon-fusion processes have been usually considered at dedicated high-energy photon-colliders

through Compton-backscattering of laser light [4], they can also be studied using the photons radiated from the e^+e^- beams. Indeed, any relativistic charged particle generates a flux of quasi-real (Weizsäcker-Williams) photons, theoretically described using the effective photon approximation (EPA) [5], which can be used for photoproduction studies. The physics of two-photon collisions has been an active topic of research at e^+e^-, proton, and ion colliders (see e.g. [6, 7] and refs. therein). The $\gamma\gamma$ kinematics can be constrained measuring the scattered leptons with near-beam detectors at low angles, while the produced system is reconstructed from its decaying products in the central detector. In this work, we are interested, first, in the $\gamma\gamma \to H$ process, considered before in the context of photon [8], proton [9] and heavy-ion [10] colliders. The huge luminosities available at FCC-ee provide the means to observe such a process which, to our knowledge, has not been studied before in e^+e^- two-photon EPA collisions. The second measurement of interest is $\gamma\gamma \to W^+W^-$, which is a very suitable process to test the electroweak sector of the SM as it probes trilinear $W^+W^-\gamma$ and quartic $\gamma\gamma W^+W^-$ boson couplings. The few counts of two-photon production of W^+W^- observed for the first time at the LHC [11, 12] have improved the limits on anomalous quartic gauge couplings (aQGC) using dimension- 6 and 8 effective operators parameters. The cleaner environment and huge luminosities of e^+e^- collisions at the FCC-ee will lead to hundreds of WW pairs observed and, thus, much more stringent aQGC limits.

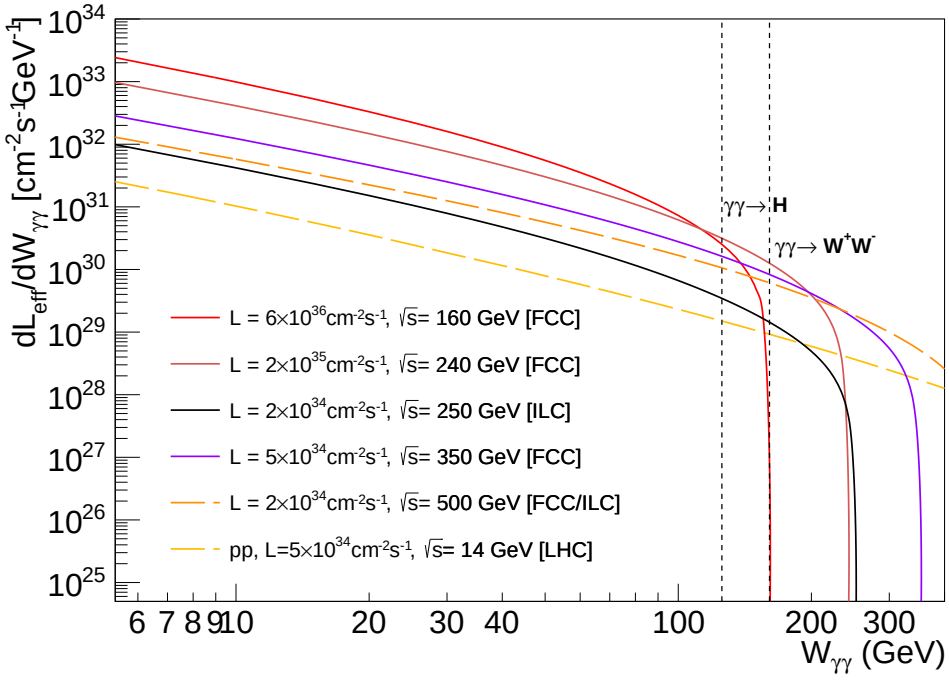

Figure 1. Effective two-photon luminosities as a function of $\gamma\gamma$ c.m. energy, from the EPA fluxes convolution at FCC-ee and ILC, and p-p at the LHC, for their nominal beam luminosities. The dashed vertical lines show the $\gamma\gamma \to H$ and $\gamma\gamma \to W^+W^-$ production thresholds.

Figure 1 shows the $\gamma\gamma$ effective luminosities $\mathcal{L}_{\rm eff}$ obtained from EPA fluxes for lepton and hadron colliders at various center-of-mass (c.m.) energies. The vertical dashed lines indicate the threshold of production for the two processes considered here. Photon-fusion Higgs production can be in principle observed at FCC-ee running at $\sqrt{s} = 160$ GeV, although the best conditions for measuring both processes are provided by e^+e^- at $\sqrt{s} = 240$ GeV. In this case, the $\mathcal{L}_{\rm eff}$ is 20 times greater than at the LHC, with the advantage of the absence of pile-up collisions.

2. Theoretical setup

All charges accelerated at high energies generate electromagnetic fields which, in the EPA approach, can be considered as quasi-real (low virtuality) photon beams. After interacting with each other, the two photons can produce various exclusive final states $e^+e^- \to e^+\gamma\gamma e^- \to e^+ X e^-$, where X is either W^+W^- or the Higgs boson in this work (diagrams in Fig. 2), and the radiated leptons are scattered at very small angles with respect to the beam direction. The production cross sections are computed in a factorized way through the convolution of the EPA photon fluxes and the elementary $\gamma\gamma \to X$ process described by exact matrix elements and kinematics. Although various Monte Carlo (MC) event generators –such as PYTHIA 6 [13], MadGraph 5 [14], WHIZARD [15] or SuperChic 2 [16]– have in principle the possibility to run $\gamma\gamma$ collisions in the EPA mode, not all production processes are available and/or the simulation of the outgoing e^+e^- kinematics is not always exact (and such information is crucial for realistic studies of the e^+e^- tagging probability). In this study, we employ two different MC codes, MadGraph 5 (version 2.1.1) and PYTHIA 6 (version 6.4.28), to study respectively Higgs and W^+W^- two-photon production.

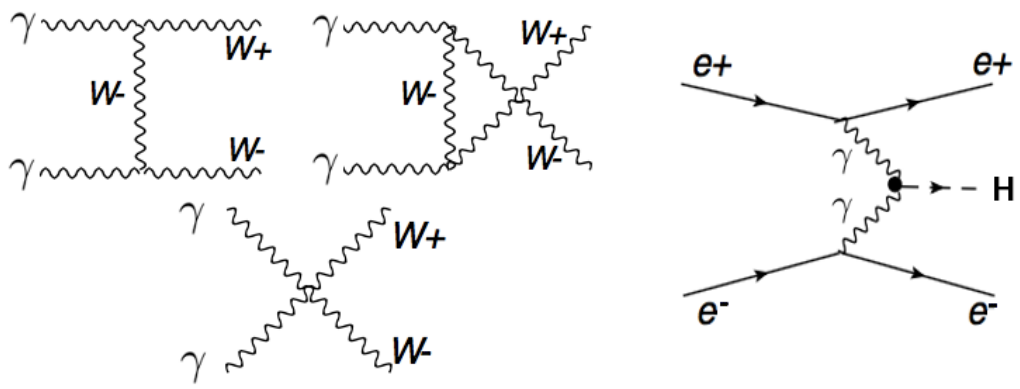

Figure 2. Diagrams for W^+W^- (left) and Higgs boson (right) γ-fusion production in e^+e^- collisions.

We run MadGraph 5 with the effective field theory (HEFT) approach, where the scalar Higgs couples directly to photons, combined with the EPA to compute the cross sections for the process $\gamma\gamma \to H \to b\bar{b}$, and the relevant continuum backgrounds $\gamma\gamma \to b\bar{b}, c\bar{c}, q\bar{q}$ (with $q = u, d, s$ being light quarks). The final-states are studied at the parton level, i.e. neither quark showering nor hadronization and decays are considered for this preliminary study (a more complete analysis is in progress). The simulated signal and background samples for $\gamma\gamma \to W^+W^- \to 4$ jets were generated using PYTHIA 6 [13] in the EPA approach (process ID=69, which properly accounts for the scattered e^+e^- kinematics) and full parton-shower and hadronization of the jets from the W decays. With both gauge bosons $W^\pm$ producing four jets in the final state, the statistics is maximized due to the higher branching ratio compared to the leptonic decay channels used in the CMS analyses in p-p at 7 and 8 TeV [11, 12].

3. Results

3.1. $\gamma\gamma \to H \to b\bar{b}$ process

The visible cross sections for $\gamma\gamma \to H \to b\bar{b}$ obtained with MadGraph 5 are $\sigma_{\gamma\gamma\to H\to b\bar{b}} = 20$ ab and 85 ab in e^+e^- collisions at $\sqrt{s}$ =160 GeV and 240 GeV respectively, assuming a 70% reconstruction/tagging efficiency for each single b-jet (which leads to a combined 50% efficiency

for the $b\bar{b}$ signal). The main backgrounds to the signal are the continuums $\gamma\gamma \to b\bar{b}$, and $\gamma\gamma \to c\bar{c}, q\bar{q}$ where the charm and light quarks are misidentified as b-quarks. Assuming b-jet mistagging probabilities of 5% for a c-quark, and 1.5% for a light-quark, effective reductions of the $c\bar{c}$ and $q\bar{q}$ continuum backgrounds by factors of about 400 and 4×10^3, respectively, are achieved. Taking all these factors into account, the backgrounds are still about 30 times larger than the signal in the region of jet-pair invariant masses 100 GeV $\leq M_{inv}^{jj} \leq$ 140 GeV around the Higgs peak, but can be safely reduced with a few kinematics cuts that are described below in detail and summarized in Table 1. Figure 3 compares the b-jets kinematical distributions for the signal and backgrounds for e^+e^- collisions at $\sqrt{s} = 240$ GeV. The kinematical distributions for $\sqrt{s} = 160$ GeV are similar and are not shown here for obvious reasons.

Table 1. Summary of the visible cross sections for signal and backgrounds for the $\gamma\gamma \to H \to b\bar{b}$ analysis, obtained from the MadGraph 5 simulations for e^+e^- collisions at $\sqrt{s} = 160$, 240 GeV, following the selection criteria described in the text.

Process	$\sqrt{s}$ (GeV)	$[M_{\rm inv}^{jj} = 100$–140 GeV/c$^2]$ (b-jet (mis)tag efficiency)	... ... $[p_T^j = 53.5$–62.5 GeV/c] $\lvert\cos\theta^j\rvert < 0.45$ $[M_{\rm inv}^{\rm jj} = 115$–$135$ GeV/c$^2]$	... ... $e^{\pm}$-tag
$\gamma\gamma \to H \to b\bar{b}$	160	40 ab (20 ab)	9.2 ab	4.6 ab
$\gamma\gamma \to b\bar{b}$		1 120 ab (556 ab)	16.2 ab	8.1 ab
$\gamma\gamma \to c\bar{c}$		21 610 ab (54 ab)	0.13 ab	0.06 ab
$\gamma\gamma \to q\bar{q}$		24 320 ab (5.5 ab)	0.002 ab	0.58e-3 ab
$\gamma\gamma \to H \to b\bar{b}$	240	170 ab (85 ab)	39.3 ab	19.6 ab
$\gamma\gamma \to b\bar{b}$		4 020 ab (2010 ab)	67.8 ab	34.0 ab
$\gamma\gamma \to c\bar{c}$		77 830 ab (195 ab)	6.0 ab	3.0 ab
$\gamma\gamma \to q\bar{q}$		87 760 ab (20 ab)	0.005 ab	0.002 ab

In order to remove the continuum backgrounds, several cuts can be applied according to the study [10] and the distributions shown in Fig. 3. First, since the transverse momenta of the Higgs decay b-jets peak at $p_T^j \approx m_{\rm H}/2$, selecting events with at least one jet within $p_T = 53.5$–62.5 GeV/c suppresses ∼95% of the backgrounds, while removing only ∼50% of the signal. Second, the two decay b-jets are emitted isotropically in the Higgs c.m. system, and their distribution in the helicity frame is peaked at $|\cos\theta| \approx 1$, i.e. emitted either roughly in the same direction as the $b\bar{b}$ pair or opposite to it, while the continuum –whose relevant Feynman diagrams have quarks propagating in the t- or u- channel– is peaked in the forward and backward directions. Thus, independently requiring $|\cos\theta| < 0.45$ suppresses ∼90% of the continuum contaminations while still keeping ∼55% of signal. Combination of both criteria enhances the (S)ignal/(B)ackground by a factor of ∼15 (if needed one could further exploit the jet pseudorapidity distributions, which are peaked around $\eta \approx 0$ for the signal and more spread out for the continuum). The final Higgs yield extraction is obtained integrating the invariant mass distribution of the jet pairs within $M_{inv}^{jj} = 115$–135 GeV/c^2, i.e. $\pm 2\sigma$ around the assumed ∼3.5 GeV per-jet energy resolution. This has no effect on the final signal but further reduces 69% of the backgrounds below the (now narrower) peak region considered. It's worth mentioning that we didn't consider any non-$\gamma\gamma$ backgrounds from $e^+e^- \to b\bar{b}$ processes. Our assumption is that all such events are removed by requiring a double-tagging condition on opposite-sign electron/positron at each side of the detector, with kinematics consistent with the reconstructed central system. We assume

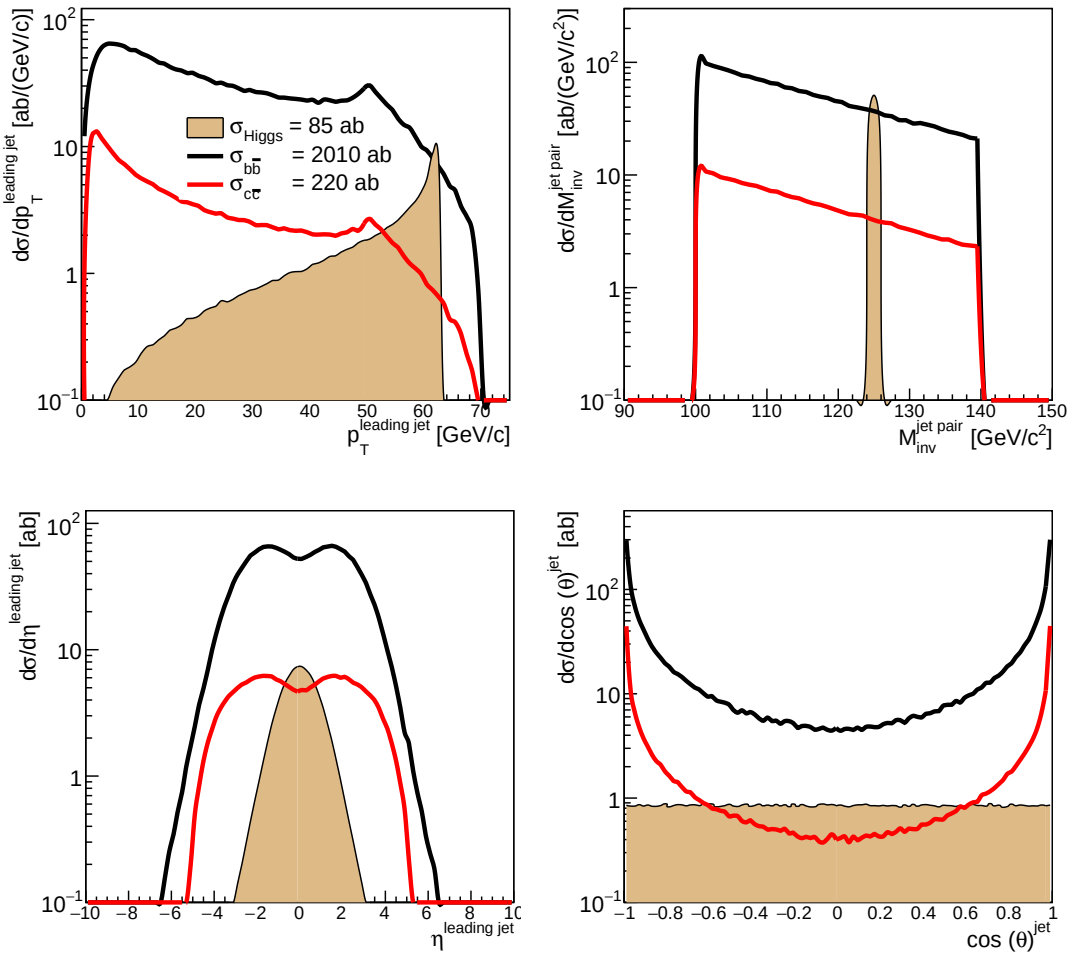

Figure 3. Kinematical distributions of the b-jets from signal (filled histograms) and backgrounds in the analysis $\gamma\gamma \to H \to b\bar{b}$ at $\sqrt{s} = 240$ GeV: transverse momentum p_T^j (top left) and pseudorapidity η^j (bottom left) of each jet; invariant mass M_{jj} of the jet pair (top right), and cosine of the angle θ between the jet, boosted to the rest frame of the pair, and the direction of the pair (helicity frame, bottom right). All distributions are normalized to their visible cross sections assuming the b-jet reconstruction and (mis)tagging efficiencies quoted in the text.

$e^{\pm}$ detection over $1^{\circ} < \theta_{e^{\pm}} < 179^{\circ}$, where $\theta_{e^{\pm}}$ is the angle of the scattered $e^{\pm}$ with respect to the beam, and 50% of efficiency for the double-tagging of $\gamma\gamma$ events. The visible cross sections remaining after application of the aforementioned selection cuts are listed in Table 1, and their impact in the final kinematical distributions are shown in Fig. 4. From the final visible cross sections listed in the fifth column of Table 1, we expect evidence ($S/\sqrt{B} > 3\sigma$) for Higgs boson production in the $b\bar{b}$ decay channel at $\sqrt{s} = 160$ GeV (240 GeV) with $\mathcal{L} = 3.5$ ab^{-1} (0.9 ab^{-1}). Full 5σ-observation of two-photon Higgs production in this decay channel would occur at $\sqrt{s} = 160$ GeV (240 GeV) for $\mathcal{L} = 10$ ab^{-1} (2.5 ab^{-1}). Both observations are thus guaranteed with the current FCC-ee plans to integrate $\mathcal{L} = 15.2$ ab^{-1} and $\mathcal{L} = 3.5$ ab^{-1} per-year at each c.m. energy in a total of four interaction points.

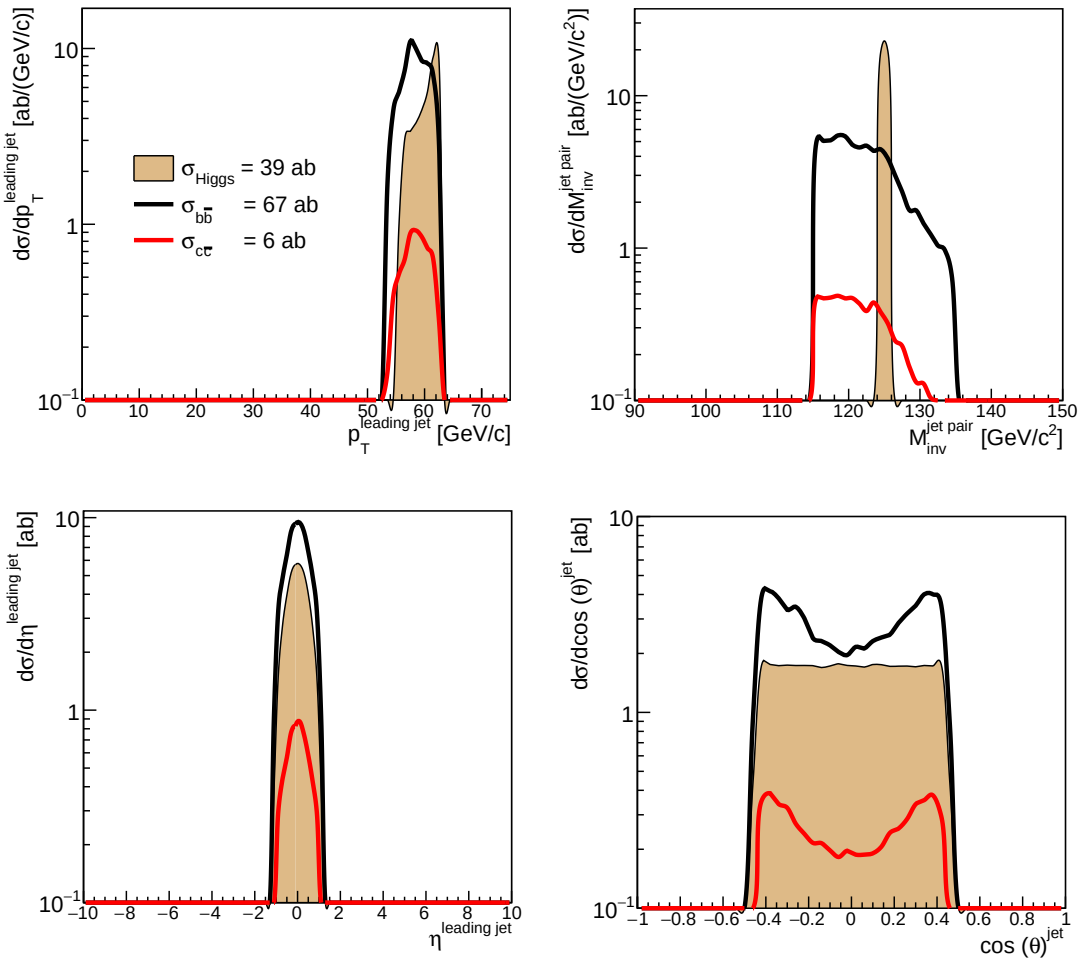

Figure 4. Kinematical distributions of the b-jets from signal (filled histograms) and backgrounds in the analysis $\gamma\gamma \to H \to b\bar{b}$ at $\sqrt{s} = 240$ GeV: transverse momentum p_T^j (top left) and pseudorapidity η^j (bottom left) of each jet, invariant mass M_{jj} of the jet pair (top right), and cosine of the angle θ between the jet, boosted to the rest frame of the pair, and the direction of the pair (helicity frame, bottom right); after application of all selection criteria mentioned in the text.

3.2. $\gamma\gamma \to W^+W^- \to$ *4-jets process*

The generation of the two-photon production of W^+W^- pairs in the fully hadronic decay channel was performed with PYTHIA 6, which predicts a cross section of $\sigma_{\gamma\gamma\to WW} = 7.23$ fb in e^+e^- at $\sqrt{s} = 240$ GeV. The dominant background from the process, $e^+e^- \to 4$ jets with very large cross sections of $\sigma \approx 8.8$ pb, should be killed with the $e^\pm$ double-tagging condition, leaving only the irreducible $\gamma\gamma \to 4$ jets process with cross section $\sigma = 25$ fb, to deal with. The e^+e^- k_T ("Durham") jet reconstruction algorithm [17] from the Fastjet package [18] has been used to perform the clustering of all the hadronic energy in the event into four exclusive jets. The transverse momentum p_T and pseudorapidity η of the leading jet, the invariant mass M_{jj} of jet pairs and the scattered angle of the outgoing leptons $\theta_{e^\pm}$ with respect to the beam are used as kinematical variables for improving the signal significance against the background. Figure 5

Table 2. Summary of the cross sections values for signal and backgrounds for the $\gamma\gamma \to W^+W^- \to$ 4-jets analysis, obtained from PYTHIA 6 simulations for e^+e^- at $\sqrt{s} = 240$ GeV, following the selection criteria described in the text.

Process	$\sqrt{s}$	Generator-level (no cut)	$p_T^j > 10$GeV/c $\lvert\eta^j\rvert < 0.5$ $\Delta R^{jj} > 0.4$	... ... $[M^{jj} = 76.5$–84.5 GeV/c$^2]$ $e^\pm$-tag
$\gamma\gamma \to W^+W^- \to$ 4jets	240	7 234 ab	5 809 ab	626 ab
$\gamma\gamma \to$ 4jets	240	24 890 ab	999.6 ab	56 ab

compares such kinematical distributions for signal and irreducible background at $\sqrt{s} = 240$ GeV, before any analysis selection applied.

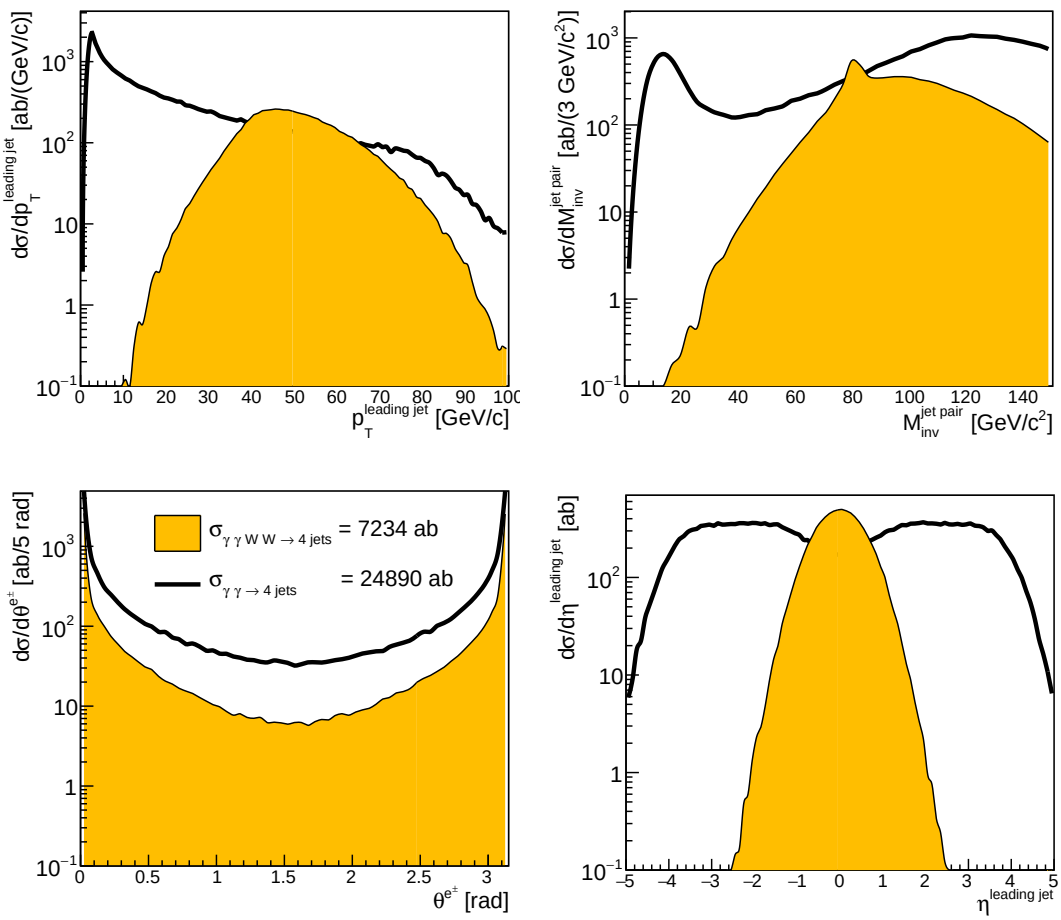

Figure 5. Kinematical distributions of signal (filled histograms) and backgrounds in the analysis $\gamma\gamma \to W^+W^- \to$ 4-jets at $\sqrt{s} = 240$ GeV: transverse momentum (top left) and pseudorapidity (bottom right) of the leading jet, invariant mass M_{jj} of jet pairs (top right) and scattered angle of the outgoing leptons (bottom left), without any selection criteria applied.

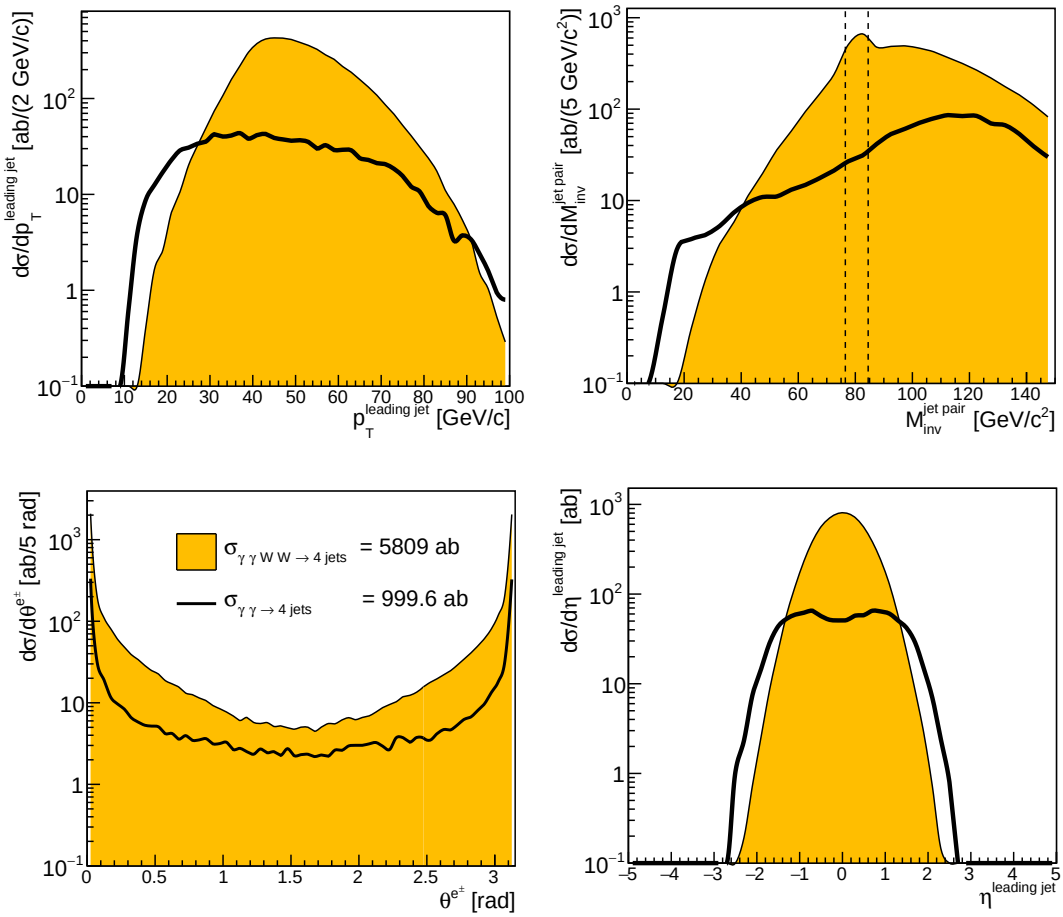

Figure 6. Kinematical distributions of signal (filled histograms) and backgrounds in the analysis $\gamma\gamma \to W^+W^- \to$ 4-jets at $\sqrt{s} = 240$ GeV after applying the acceptance cuts ($p_T^j > 10$ GeV, $|\eta^j| < 5$ and $\Delta R^{jj} > 0.4$): transverse momentum p_T^j (top left) and pseudorapidity η^j (bottom right) of the leading jet; invariant mass M_{jj} of the jet pair (top right), and scattered angle of the outgoing leptons (bottom left).

Assuming basic detector acceptance cuts: four exclusive jets reconstructed with $p_T^j > 10$ GeV, $|\eta^j| < 5$ and $\Delta R^{jj} > 0.4$, reduces ∼90% of the continuum background against only ∼20% of the signal. The corresponding kinematical distributions are plotted in Figure 6. In addition, we assume the tagging of both scattered leptons, within the polar angle acceptance range $1^\circ \leq \theta_{e^\pm} \leq 179^\circ$, with a 50% efficiency. The last selection criterion required for improving our signal to background ratio, is an invariant mass of the jet pairs around the $W^\pm$ mass, i.e. within the 76.5 GeV $\leq M_{jj} \leq$ 84.5 GeV mass window. The combined application of all selection cuts leads to a suppression of a factor of ∼10 of the signal events, and a ×450 reduction of the irreducible background. For an integrated luminosity of $\mathcal{L} = 1$ ab^{-1}, we expect more than 600 events for the signal, i.e. 10 times above the number of irreducible background counts, reaching a signal-to-background ratio of $S_{\gamma\gamma\to WW\to 4jets}/B_{\gamma\gamma\to 4jets} \approx 11$, and a statistical significance of $\mathcal{S} \approx 25$ obtained with a method based on a profile likelihood ratio [19]. As a matter of fact, the simple (5σ) observation of $\gamma\gamma \to WW \to 4$ jets would just require $\mathcal{L} = 0.05$ ab^{-1} at $\sqrt{s} = 240$ GeV, although strict aQGC tests will profit from the much larger statistical signal expected with the full integrated luminosity.

4. Conclusions

We have presented feasibility studies for the observation of two-photon production of the Higgs boson (in the $b\bar{b}$ decay channel) as well as W^+W^- pairs (in their fully-hadronic decay mode) in e^+e^- collisions at the FCC-ee, using the equivalent photon flux of the colliding beams. Both final-states are otherwise inaccessible at the LHC due to the huge backgrounds in their full-jet decay channels. Results are presented for collisions at center-of-mass energies of $\sqrt{s} = 160$ GeV and 240 GeV using MadGraph 5 and pythia 6 Monte Carlo simulations based on the EPA approach. Realistic jet acceptance and reconstruction efficiencies are applied as well as selection criteria to enhance the signals over the relevant backgrounds. In the case of the W^+W^- analysis, parton-showering and hadronization from pythia 6 is combined with the Durham algorithm for clustering of the hadronic energy into four exclusive jets.

Observation of both processes at the 5σ-level is achievable for the expected FCC-ee luminosities. The measurement of $\gamma\gamma \to WW \to 4$ jets will yield more than 600 final counts which will allow for detailed studies of the trilinear $WW\gamma$ and quartic $\gamma\gamma WW$ couplings, either in the standard model or assuming new physics scenarios in terms of dimension-6 and 8 effective operators [12]. Extraction of limits on anomalous quartic gauge couplings from these simulations requires more advanced phenomenological studies since higher-dimension effective operators using photon fluxes depend strongly on new implementations in the MC generator tools. A full simulation (including geant-based detector response) of both processes would provide more realistic conditions which are, however, beyond the scope of these proceedings and should not change its main conclusions. The feasibility analyses developed in this work confirm the unique Higgs and electroweak physics potential open to study in $\gamma\gamma$ collisions at the FCC-ee.

Acknowledgments

P. R. T. thanks Photon'15 and the CMS Collaboration for financial support. This work has granted partially by the Brazilian Science without Borders Program from Coordination for the Improvement of Higher Education Personnel – CAPES (contract BEX 11767-13-8).

References

[1] ATLAS Collaboration, Phys. Lett. **B716**, 129 (2012); CMS Collaboration, Phys. Lett. **B716**, 3061 (2012).
[2] B. Benedikt, B. Goddard, D. Schulte, F. Zimmermann and M. J. Syphers, IPAC-2015-TUPTY062.
[3] TLEP Design Study Collaboration, JHEP **01**, 164 (2014).
[4] V. I. Telnov, Nucl. Instrum. Meth. A **355**, 3 (1995).
[5] V. M. Budnev et al., Phys. Rept. **15**, 181 (1974).
[6] D. d'Enterria, M. Klasen and K. Piotrzkowski, Nucl. Phys. Proc. Suppl. **179-180** (2008).
[7] A. J. Baltz *et al.*, Phys. Rept. **458**, 1 (2008)
[8] S. J. Brodsky and P. M. Zerwas, Nucl. Instrum. Meth. A **355**, 19 (1995).
[9] V. A. Khoze, A. D. Martin and M. G. Ryskin, Eur. Phys. J. C **23**, 311 (2002).
[10] D. d'Enterria and J. Lansberg, Phys. Rev. **D81**, 014004 (2010).
[11] CMS Collaboration, JHEP **1307**, 116 (2013).
[12] CMS Collaboration, CMS PAS FSQ-13-008 (2014).
[13] T. Sjostrand, S. Mrenna and P. Skands, JHEP 0605:026 (2006).
[14] J. Alwall et al., JHEP **0709**, 028 (2007).
[15] W. Kilian, T. Ohl and J. Reuter, Eur. Phys. J. C **71**, 1742 (2011).
[16] L.A. Harland-Lang, V.A. Khoze, M.G. Ryskin, arXiv:1508.02718 (2015).
[17] S. Catani, Y.L. Dokshitzer, M. Olsson, G. Turnock and B.R. Webber, Phys. Lett. **B 269**, 432 (1991).
[18] M. Cacciari, G. P. Salam and G. Soyez, Eur. Phys. J. **C72**, 1896 (2012).
[19] G. Cowan, arXiv:1307.2487 [hep-ex] (2013).